Thermal Design and Heat Transfer Analysis of Heat Sinks and Enclosures: A Review

Ahmed Dhafer Abdulsahib[1]* , Dhirgham Alkhafaji[1] , Ibrahim M. Albayati[2]

[1] Mechanical Engineering Department, University of Babylon, Babylon 51001, Iraq
[2] School of Engineering and Physical Sciences, Heriot Watt University, Edinburgh EH14 4AS, UK

Corresponding Author Email: ahmed.abdel-saheb.engh465@student.uobabylon.edu.iq

ABSTRACT

Heat sinks are used as heat exchangers to dissipate heat from electronic equipment due to their high functionality and viability. However, heat dispersion is the main obstacle to improving the heat sinks thermal efficiency. This paper has two main parts. The first part of this study focuses on the thermal design of the heat sink, encompassing several factors such as heat dissipation devices using natural convection, heat sinks with various geometries, locations of intake and outlet, materials of the core, flat fins (especially FPFHS and PFHS fins), and porosity fins. Heat sinks that are single-layered or multi-layered and heat sinks that use different cooling liquids. The second part examines interior heat transmission by investigating various indoor geometries, including cylindrical, circular, rectangular, and hexagonal shapes, and assessing their effect on the transport of heat. Additionally, interior structures influence various fin arrangements for any type of heat convection, including actual trials conducted on enclosures using diverse fin designs, are considered. The current study aims to collect research literature that studies the heat sink and various enclosures. The research has been divided into groups to simplify the research process for activities that use cavitation-based technology to improve heat transfer for heat sinks, especially heat exchangers used to cool electrical equipment. These advantages can be attributed to their outstanding features, which include ease of production, cost-effectiveness, and effective heat dissipation.

1. INTRODUCTION

Heat sinks have been researched as a viable method for cooling electronic equipment due to their convenient production process and affordable price. Dissipaters are designed with extended surfaces that include either flat fins or pins. With the progress of technology and the miniaturization of electronic equipment, there has been a rise in the use of liquid coolants. Heat sinks are employed in industrial settings to dissipate excess heat. Recent research emphasizes the influence of fin forms and arrays of heat sinks on flow properties and thermal efficiency [1].

Conversely, several approaches were examined to enhance heat transmission in enclosed spaces, including spacers, augmenting boundary thickness, and introducing fins to the cavities. Research papers aim to improve heat transmission's thermal efficiency in these cavities by computational and experimental methods. It involves exploring various geometries and fluid types used in the process.

A thorough examination of techniques for improving heat sink thermal design has been done. The research covers different ways to improve heat sink heat dissipation [2, 3]. Examined the impact of various microchannel geometries on heat transmission and pressure drop and provided a concise overview of the kinds of fluids used [4, 5]. Furthermore, an evaluation has been conducted on heat sinks designed to cool electrical devices in commercial settings [6, 7]. The impact of various factors such as orientation, forms, holes, slots, discontinuities, fin spacing, and arrangement on heat sinks' performance under free and forced convection circumstances was analyzed [8]. A comprehensive summary of experimental studies on fluid flow behavior via heat sinks has been provided [9]. Microchips are producing more heat as a result of the quick advancement of technology. Specifically, the average heat flux of the chips has risen from around (50 W/cm²) in 2010 to over (250 W/cm²) in 2012 [10, 11].

Heat transfer in cavities and different numerical models that investigated the impact of many parameters, such as the Rayleigh, Hartmann, and Darcy numbers, were demonstrated. It also considers other factors like angle of inclination, number of ripples, and the presence of an internal body [12]. The review covered heat transport studies in cavities of different shapes using experimental, and numerical methods [13]. It also examined the impact of factors such as the nanofluid's volume fraction, the porous layer's thickness, the number of ripples, and the existence of an internal body with various shapes [14]. The examination encompasses a broad spectrum of experiments investigating containers with various geometric designs and numerous kinds of liquids [15-17]. Triangular, C-shape, concentric annulus, hemispherical, and parallelogrammical forms have also been studied to improve convective heat transfer [18-20].

Electronic devices have advanced significantly as a result of the remarkable advancements in technology in recent years.

As the complexity and efficiency of these devices increased, the urgent need to reduce the heat generated by their operation emerged. Excessive heat is one of the biggest challenges the electronics industry faces, as it can negatively affect performance and reduce the life of electronic components. Previous research has focused on optimizing heat transmission in heat sinks and cavities. Still, detailed inquiries into heat transfer in heat sinks, specifically inside cavities, have been lacking. Hence, the objective of the present investigation was to review research papers related to heat sinks and cavities and classify them based on their type of study. Therefore, this paper will give researchers a thorough overview, enabling them to explore enhanced heat transfer processes in heat sinks using cavitation-based approaches.

2. THERMAL DESIGN OF HEAT SINKS

This section compiles published studies on heat sinks, focusing on their diverse designs and the magnitude of their influence on heat transmission.

2.1 Thermal dissipaters using natural convection

Tari and Mehrtash [21] studied the heat analysis in finned heat sinks at different tilt angles ±60°, ±75°, +80°, ±85°, and ±90° from vertical by changing gravitational acceleration by several up-and-down inclinations to determine flow arrangements around heat sinks. Nusselt number correlations for all pitch angles were accurate within 20% when fin spacing values were near the optimal. Tari and Mehrtash [22] examined inclined heat sink steady natural convection. The examined inclination angles were found acceptable for cooling electronic equipment, and the hypothesized correlations are useful in electronics cooling. Jang et al. [23] examined the directional impact of a cylindrical LED light bulb heat sink. The direction impact increased with fin length and number of fins, while fin height had little influence. A correlation is presented by the Nusselt number around a cylindrical heat sink. Figure 1 displays heat sinks with varying designs to illustrate their impact on natural convection. Muneeshwaran et al. [24] suggested a central hole heat sink to improve horizontal natural convection heat transmission. The results showed that a heat sink with emissivity (0.9) lowered thermal resistance by 23% above (0.15).

2.2 Different designs of heat sinks

Hung and Yan [25] created a tapered channel to increase microchannel heat sink thermal performance. When pumping power is more significant than 0.4 W, the MCHS with tapered-width channel design improved thermal performance by 16.7% over the parallel channel design. The heat sink cools the LED bulb to keep its maximum temperature in contact with it below the manufacturer's critical temperature. Costa and Lopes [26] presented a numerical analysis on improving the heat sink for a natural convection LED lamp. Findings indicate the relation impact of various major factors on heat sink work and enable optimal solution selection within dimensional limitations. A Volume Average Theory model was used to optimize the fins by Kim [27]. The branching fin heat sink has 30% lower thermal resistance than the rectangular fin heat sink for water cooling. Reduced heat sink length and pumping power improve the decrease. To provide additional

illustration, several forms of heat sinks were selected in Figure 2, which depicts the impact that these heat sinks have on heat transmission when different parameters are introduced. Türkakar and Okutucu-Özyurt [28] and Shahsavar et al. [29] improved the dimensions of the heat sink by reducing the thermal resistance.
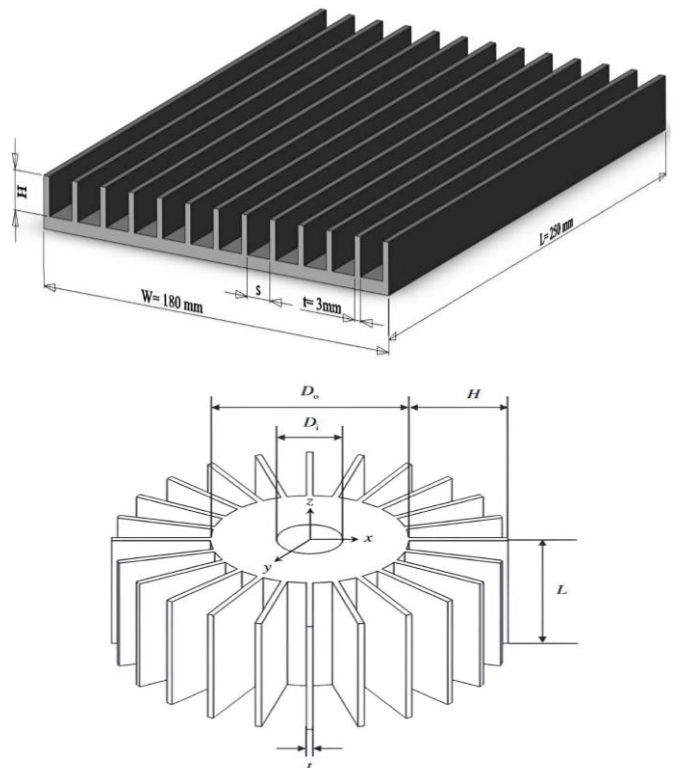
Figure 1. Various heat sink designs [21, 23]
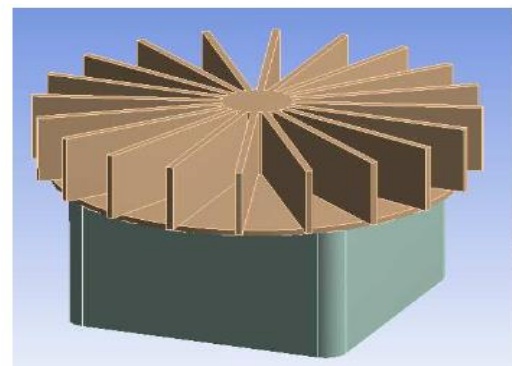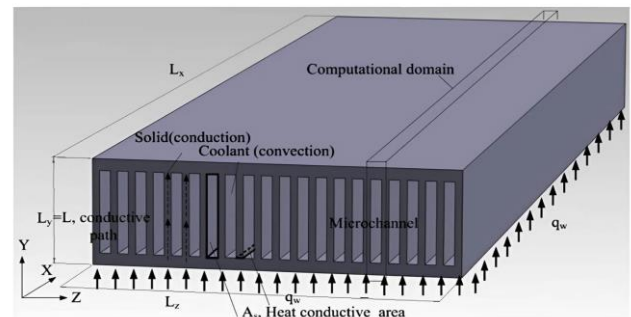
Figure 2. Various heat sink designs with different factors [25, 26]

2.3 Variations in inlet and outlet locations for heat sinks

Vinodhan and Rajan [30] performed computational studies for heat sink (MCHS). New designs have lower thermal resistances than standard MCHS at the same pumping power. Changes in channel dimensions may improve the design. Xia et al. [31] showed that type I has greater flow velocity uniformity than type Z. Type I flow distribution is symmetrical. Heat sink C also has better heat transfer properties for $q_v = 150$ ml/min and can extend the life of microelectronic devices. Al-Hasani and Freegah [32] investigated the hydrothermal performance of three microchannel serpentine heat sinks (MCHS) numerically and experimentally. Model B has superior temperature distribution, maximum core temperature, Nusselt number, and thermal resistance compared to Model A.

2.4 Diverse substrate materials for heat sinks

Mohammed et al. [33] used several core nanofluids to study MCHS laminar flow and heat transmission numerically. Water-based nanofluids may increase heat transfer in steel substrate heat sinks. Qu et al. [34] created electronic thermal management. The hybrid heat sink has sintered parallel fins on top and a hollow bottom filled with copper mineral foam and paraffin. They found that when the porosity of the metal is reduced, the surface temperature decreases. Shkarah et al. [35] detailed micro-channel heat sink numerical calculations. Graphene reduces thermal resistance best for heat transmission. These findings led to graphene's study as a micro-channel heat sink substrate.

2.5 Heat sinks have flat-plate fins, including FPFHS and PFHS

Lin et al. [36] increased heat transfer surfaces in CPU cooling heat sinks with vertical flat fins. A $70\times70\times15$ mm³ high-pressure axial flow fan integrates with vertical and inclined fins to create heat sink collectors. CPU emulators used 82 watts. Testing demonstrates that heat sink assemblies with ready planar fins perform better than vertical fin assemblies owing to their bigger surface area and faster flow. Adding angled fins to a 2000 RPM high-pressure fan may lower CPU temperature by 6℃. Zhao et al. [37] improved square-fin micro heatsinks to outperform micro-column fin ones in thermal performance. Al-Sallami et al. [38] found the perforated SFHSs minimize processor temperatures and mechanical power consumption for practical microelectronics cooling applications.

2.6 Porous media heat sink implementation

Hung et al. [39] quantitatively examined how channel outlet expansion affects microporous channel heat sink (MCHS) heat transfer. Thus, increasing the channel outlet width or height expansion ratio improves porous MCHS hydraulic and thermal performance. Zhang et al. [40] constructed a novel microchannel heat sink using porous metals with large cylindrical holes generated. The base metal was copper because of its excellent heat conductivity. Cutting copper into four or eight identical pieces aligned in the pore axis increases the heat transfer coefficient to 9 W/(cm² K). Jeng and Tzeng [10] fused 0.5-0.85 mm copper beads perfectly with a copper heat sink's radial plate fins in thin layers at high temperatures to create an LED cooler with metal bead layer fins. The study

found that B and C had twenty-six percent and sixteen percent greater thermal resistance than Model A at $\Delta T \fallingdotseq 30℃$ and pure heat. Model B has 31% lower thermal resistance in mixed convective heat transfer than Model A. Deng et al. [41] used conventional sintering to create a porous heat sink with re-entrant microchannels. The re-entry porous microchannels reduced wall temperature increase for boiling and delayed and eased two-stage flow instability. Liu et al. [11] carefully evaluated the heat impact of heat sink under varied structural and hydrodynamic factors using Fluent-3D numerical simulation. The perfect pore diameter for the water coolant was smaller (0.1-0.2 mm) and had the same porosity as the GaInSn coolant at the same pressure drop. Abdollahi et al. [42] found that increasing the volume ratio of nanoparticles in the hybrid mixture lowers the solid and hybrid nanofluid surface temperatures and enhances Brownian motion. As the Darcy number rises, the solid sections and Cu: AlOOH/water thermal fields improve.

2.7 Diverse working fluids in heat sinks

Ho and Chen [43] investigated forced convection heat transfer in a microcopper heat sink using Al_2O_3/aqueous nanofluid instead of pure water. Average heat transfer coefficients were calculated using the inlet and bulk temperature differential and Reynolds numbers from 133 to 1515. Moraveji et al. [44] aimed to find new numerical and experimental approaches to regulate heat load to enhance information technology (IT). The influence of nanoparticle percent on the coefficient of heat transmission at various Re was also explored. The linked equations for Nu that found with satisfactory precision using modeling findings. Moraveji and Ardehali [45], Ho et al. [46], and Naphon and Nakharintr [47] demonstrated that suspended nanoparticles significantly improve heat transfer.
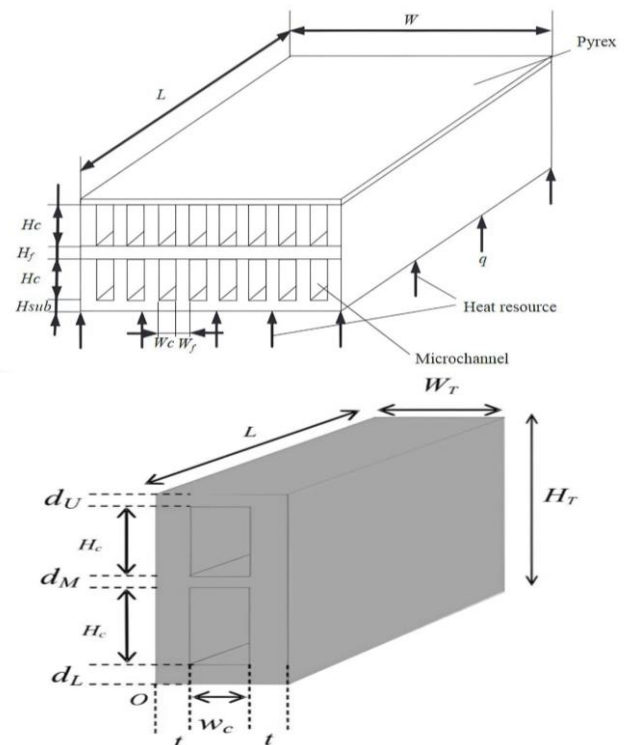
Figure 3. A schematic diagram for the use of layered heat sinks [48, 49]

2.8 Single or double-layer heat sinks

Shao et al. [48] optimized the multi-layer microchannel heat sink arrangement sizes to increase the 556 W/cm² high-flow chip performance. The most significant ΔT=77°C, while the transmitted power of heat flow is 200W. Therefore, the heat resistance =0.3893°C/W, which matches the thermal resistance network model study. Wong and Muezzin [49] used computational analysis to forecast the thermal performance of a two-layer ultra-fine heat sink with parallel heat transfer and compare it to opposing flow for various channel aspect ratios. To elucidate the heat sinks that are utilized in the process of constructing many layers, the research presented in Figure 3 was selected to provide a clear image of the utilization of these models.

Ahmed et al. [50] and Ho et al. [51] demonstrated that double-layer, microchannel heat sinks are better for engineering applications than single-layer ones. A review that focuses on the thermal design of heat sinks is summarized in Table 1.

Table 1. Summary of heat sink thermal design assessment

Authors	Configuration	Parameters	Method	Main Results
Thermal Dissipaters Using Natural Convection				
Tari and Mehrtash [21]	Finned heat sinks	Tilt angles	Experimental & Numerical	Nusselt number correlations for all pitch angles are accurate within 20% when fin spacing values are near the optimal
Tari and Mehrtash [22]	Aluminum heat sinks	Heat transfer rate sensitivity	Experimental & Numerical	The researched parameter ranges are acceptable for cooling electronic equipment, and the hypothesized correlations are useful in electronics cooling
Jang et al. [23]	Cylindrical LED light bulb heat sink	Inclination angle	Experimental & Numerical	The direction impact increased with fin length and number of fins, while fin height had little influence
Muneeshwaran et al. [24]	Heat sink with a central hole	Heat sink thermal behavior and airflow	Experimental & Numerical	Heat sink with an emissivity of 0.9 reduced thermal resistance by 23% compared to 0.15
Different Designs of Heat Sinks				
Hung and Yan [25]	Microchannel heat sink	Temperature distribution and resistance	Numerical	Tapered-width channel design improved thermal performance by 16.7% over the parallel channel design
Costa and Lopes [26]	Heat sink cools the LED bulb	Maximum temperature and fin number, length, and height	Numerical	The relative impact of various governing factors on heat sink performance and enable optimal solution selection
Kim [27]	Heat sink with branching fins	Average volume	Numerical	The branching fin heat sink has 30% lower thermal resistance than the rectangular fin heat sink for water cooling
Türkakar and Okutucu-Özyurt [28]	Silicon microchannel heat sink	Thermal resistance	Numerical	Optimized various local heat sources and uniform convection
Shahsavar et al. [29]	Spiral heat sink	Reynolds numbers and platelet particles	Numerical	Laminar and turbulent flow increase 6.32-fold, most with platelet nanoparticles
Variations in Inlet and Outlet Locations for Heat Sinks				
Vinodhan and Rajan [30]	Microchannel heat sink (MCHS)	Flow and temperature transmission	Numerical	New designs have lower thermal resistances
Xia et al. [31]	Microchannel heat sinks with different inlet/outlet locations	Flow velocity uniformity	Numerical	Head forms rectangle heads provide higher movement speed homogeneity
Al-Hasani and Freegah [32]	Three microchannel heat sinks (MCHS)	Hydrothermal performance	Experimental &Numerical	Model B has superior temperature distribution, maximum core temperature, Nusselt number, and thermal resistance compared to Model A
Diverse Substrate Materials for Heat Sinks				
Mohammed et al. [33]	Steel substrate heat sinks	Examined water, ethylene glycol (EG), oil, and glycerol	Numerical	Glycerol-based nanofluid had the best heat transfer coefficient and temperature homogeneity across the four mixed flows, followed by oil, EG, and water
Qu et al. [34]	Hybrid heat sink	Heat dissipation methods	Experimental	Reducing foam porosity or pore density lowers surface temperature
Shkarah et al. [35]	Micro-channel heat sink	Volumetric flow rates	Numerical	Graphene reduces thermal resistance and is best for heat transmission.
Heat Sinks Have Flat-Plate Fins, Including FPFHS and PFHS				
Lin et al. [36]	CPU cooling heat sinks	Planar and vertical fins	Experimental	Adding angled fins to a 2000 RPM high-pressure fan may lower CPU temperature by 6°C
Zhao et al. [37]	Heat sink with square fins	Angle and porosity of fins	Numerical	Square fins of heat sink thermal performance depend on porosity and angle
Al-Sallami et al. [38]	Transverse-fin heat sinks	Relative cross-sectional area	Numerical	Perforated SFHSs minimize processor temperatures and mechanical power consumption for practical microelectronics cooling applications

Porous Media Heat Sink Implementation				
Hung et al. [39]	Microporous channel heat sink (MCHS)	Channel outlet expansion	Numerical	An increased channel port improves average Nusselt number, heat transport, and temperature management while reducing thermal resistance
Zhang et al. [40]	Microchannel heat sink	Porous metals with large cylindrical holes	Experimental	The water-cooled porous copper heat sink has good heat transfer
Jeng and Tzeng [10]	Copper heat sink	LED cooler with metal bead layer fins	Experimental	Model B has 31% lower thermal resistance in mixed convective heat transfer than Model A
Deng et al. [41]	Porous heat sink with re-entrant microchannels	Fourteen tiny parallel lanes	Experimental	The re-entry porous microchannels reduced wall temperature increase for boiling and delayed and eased two-stage flow instability
Liu et al. [11]	Porous copper heat sink	Varied structural and hydrodynamic factors	Numerical	The best heat sink porosity and pore diameter for the greatest equivalent heat transfer coefficient
Abdollahi et al. [42]	Mini/microchannel heat sinks	Nusselt number and Darcy number	Numerical	Increasing the volume ratio of nanoparticles in the hybrid mixture lowers the solid and hybrid nanofluid surface temperatures.
Diverse Working Fluids in Heat Sinks				
Ho and Chen [43]	Microcopper heat sink	Temperature differential and Reynolds numbers	Numerical	Nanofluid-cooled heat sinks outperform water-cooled ones due to more significant average heat transfer coefficients
Moraveji et al. [44]	Microchannel heat sinks	TiO_2 and SiC nanoparticles and Reynolds numbers.	Experimental & Numerical	The influence of ϕ percent on coefficient of convective temperature transmission at various Reynolds numbers
Moraveji and Ardehali [45]	Microchannel heat sink	Φ and Re	Numerical	temperature transmission improvement has been researched to nanoparticle concentration and Reynolds number
Ho et al. [46]	Microchannel heat sink	Reynolds number, nanoparticle, and MEPCM mass fractions	Experimental	Water-based suspension efficiency in the microchannel basin correlated well with unrelated dimensional metrics in the overall figures
Naphon and Nakharintr [47]	Microchannel heat sink	Nanofluids and Reynolds numbers	Numerical	Suspended nanoparticles significantly improve heat transmission
Single or Double-Layer Heat Sinks				
Shao et al. [48]	Multi-layer microchannel heat sink	Thermal resistance network and pumping power	Numerical	Heat resistance equals 0.3893°C/W, matching the structure of the network analysis
Wong and Muezzin [49]	Two-layer ultra-fine heat sink	Reynolds number and channel aspect ratio	Numerical	Two-layer parallel-flow microchannel heat sink with a reduced middle rib thickness has a lower thermal resistance
Ahmed et al. [50]	Rectangular and triangular heat sink	Varying channel diameters, nanoparticle concentrations	Experimental	TDLMCHS has lower heat resistance than RDLMCHS
Ho et al. [51]	Double-layer micro-channel heat sink	Pressure drop and heat transfer	Experimental	The double-layer microchannel heat sink reduces pressure drop greatly compared to the single-layer heat sink

3. ENCLOSURE HEAT TRANSFER ANALYSIS

3.1 Variable geometry enclosures

This section focuses on research that examines cavities with various geometries.

3.1.1 Circular enclosure

Hatami et al. [52] investigated nanofluid heat transfer in a corrugated circular chamber via natural convection. Results demonstrate that the Le number substantially influences the Nu at greater Nr but essentially none at lower Hadavand et al. [53] found when increasing the angle of attack to 45° and 90°, the Nusselt number dropped by almost 40%. Sheikholeslami et al. [54] examined magnetizable MWCNT-Fe_3O_4/H_2O hybrid nanofluids in a circular cavity with two heaters. The findings reveal that MWCNT-Fe_3O_4 hybrid nanoparticles in the host fluid boost convective heat transfer. Gangawane and Oztop [55] investigated mixed convection in a two-dimensional semicircular cavity. Mass reduces cavity

convection heat transmission. Shahrestani et al. [56] Calculated the natural heat transfer in a circular container with a flexible wall. The average Nusselt number increases more than five times when Ra rises from 10^4 to 10^7. Raising Pr from 0.71 to 200 will raise plate pressure by almost 70 times. The research presented in this section was selected and compiled in Figure 4 to provide a more accurate depiction of the forms used in the investigation.

3.1.2 Cylindrical enclosure

An upward-facing isothermal cylindrical hollow was examined by Shen et al. [57] for convection. The findings were compared to no wind. Convective heat loss reduces and subsequently rises as wind speed increases from zero in most instances. The wind angle of incidence to maximize coupled convective heat loss depends on cavity inclination angle and wind speed. Bouhal et al. [58] simulated the melting of a phase change material (PCM) in a cylindrical chamber with heating sources using 2D CFD models. The fin structure increased heat transmission and PCM melting time. Vjatkin et al. [59]

investigated the thermal convection of a heat-generating fluid in a revolving horizontal cylinder. Heat transmission depends on vibration characteristics in resonant fluid oscillations with equal frequencies. Convection relies on vibration and centrifugation. Transverse vibrations manage rotational system heat load well. Al-Rashed et al. [60] explored the convection of nanofluids with aluminum oxide in a cover cavity with a center elliptical shape. The Nu rose 45 at ϕ equal 0.2%, and the fluid was 1.7 and 0.3. Daabo et al. [61] examined the impact of cylindrical cavity thermal receiver shape on small-scale solar Brayton cycle performance. The heat transfer coefficient was reduced by 23%, improving the shape's thermal performance.
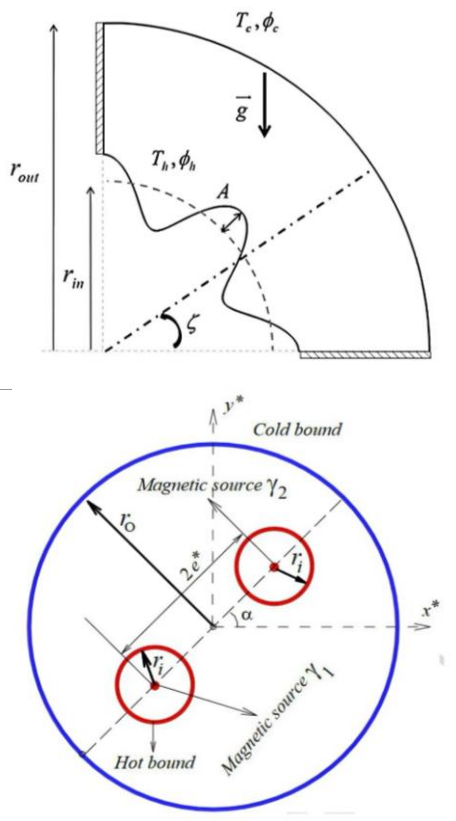
Figure 4. Schematic diagrams of the physical model [52, 54]

3.1.3 Hexagonal enclosure

Ali et al. [62] numerically modeled hexagonal cavity mixed hydrodynamic-magnetic thermal flow. It is found that the Hartmann and Richardson numbers affect flow structure and temperature field. Rehman et al. [63] used numerical methods to analyze heat transfer of fluid flow in an enclosure with a hexagonal shape. The hexagonal hollow bottom wall evenly holds the fins. Examined how the Rayleigh number affects heat transport along the heated fin surface. Increased Rayleigh number improves heat transport along the T-shaped fin surface. Haq et al. [64] modeled the hexagonal water-filled chamber with a lid numerically. Heat transfer significantly correlates with heat duration, Richardson number, and Reynolds number. Ghalambaz et al. [65] investigated the heat and mass transport behavior of nanofluids in a hexagonal container with a non-uniform magnetic field, taking into consideration ferrohydrodynamic and magnetohydrodynamic influences. Increasing the magnetic number rises temperature and mass transmission. Increased Hartmann number due to decreased heat and mass transport. Aly et al. [66] explored magnetic effects on NEPCM convection in a porous ring. The

annulus' temperature, concentration, and heat capacity circumference Cr increases with Ra. Figure 5 is an illustration of the hexagonal forms that were used in the research. This figure depicts the schematic shape that was utilized in the investigation. Aly et al. [67] found that increased Ha and decreased Da minimize nanofluid movements within the ring. Rayleigh number force promotes ring nanofluid movements. Ikram et al. [68] found that heat transfer effectiveness is contrariwise related to Bi and Ra numbers and improves considerably with Reynolds numbers. High Reynolds numbers also diminish the degree of the energy spectrum. Ahmed and Raizah [69] wanted to analyze the second law of thermodynamics for nanofluids with non-Newtonian force laws between polygonal/polygonal or polygonal/cylinder forms. The major findings showed flow area and power law control in convection and heat transfer.
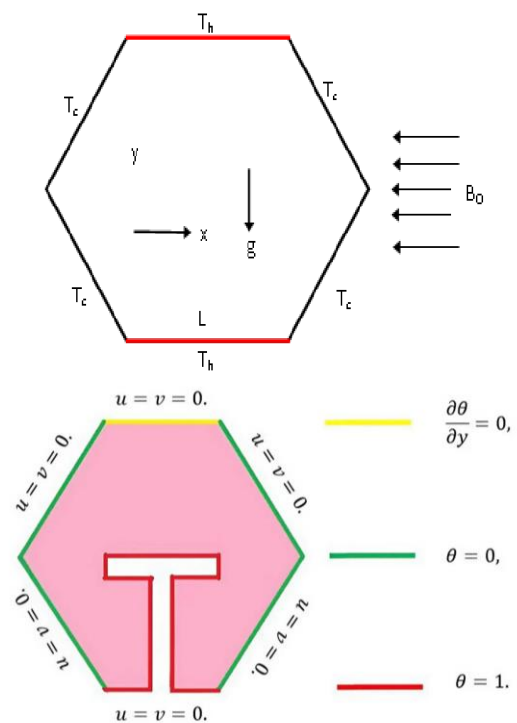
Figure 5. Schematic hexagonal design [62, 63]

3.1.4 Rectangular enclosure

Elsherbiny and Ismail [70] examined how cavity size and inclination angle affect air laminar convection in inclined rectangular cavities with two local heat sources. Increasing Φ beyond 60° reduces Nu until it reaches its minimal value at 180°. Li and Tong [71] found that increasing the cavity's aspect ratio and inclination accelerates natural convection flow and convective heat transfer. Qi et al. [72] found increasing Reynolds and Stefan numbers improve dissolution. Li et al. [73] visualized the melting of NePCM in a differentially heated rectangular chamber. Because the shorter characteristic length limits natural convection, narrower cavities can fully use enhanced heat conductivity. Thiers et al. [74] examined the numerical heat transfer effects of one or two modest heat engines. Heat transfer is best at Seventy percent of plate height. A computer study by Li et al. [75] examined the convective heat transfer pattern of molten phase change material (mPCM) in a narrow rectangular cavity with a constant heat flow boundary state on one side and a flow boundary state on the other. Increasing Ra or Re improves convective heat transfer efficiency. Qin et al. [76] found the

melting process has three phases, with Re governing the first two and Ra the final. In Table 2, which provides a concise summary of the study, a review that examines heat transmission in enclosed spaces is summarized.

Table 2. An overview of how heat is distributed through enclosed spaces

Authors	Configuration	Main Parameters	Method	Main Results
Circular Enclosure				
Hatami et al. [52]	Corrugated circular chamber	Rayleigh number, Lewis number, ratio number	Numerical	The Le substantially influences the Nu at higher Nr but essentially none at lower Nr
Hadavand et al. [53]	Cover-driven cavity's	Richardson number and semicircular cavity angle of attack	Numerical	The cavity entrance angle changed the heat transfer process
Sheikholeslami et al. [54]	A circular cavity with two heaters	Heater location angle, magnetic force ratio, magnetic number, Hartmann number	Numerical	The water with MWCNT-Fe_3O_4 duo boosts heat transfer.
Gangawane and Oztop [55]	Semicircular cavity	Richardson numbers and Grashoff numbers	Numerical	A mass with adiabatic properties was put into the cavity to minimize convection.
Shahrestani et al. [56]	A split circular container	Ra and Pr	Numerical	The average Nusselt number increases more than five times when Ra rises from 10^4 to 10^7
Cylindrical Enclosure				
Shen et al. [57]	Hollow cylindrical	Surface temperature, cavity inclination angle, wind incidence angle	Numerical	The wind angle of incidence to maximize coupled convective temperature loss is contingent on the cavity inclination direction and wind speed
Bouhal et al. [58]	A cylindrical chamber	Coefficient of Heat transmission at the sources of warming.	Numerical	The fin structure enhanced heat transfer
Vjatkin et al. [59]	A revolving horizontal cylinder	Vibration frequency and rotation frequency	Experimental & Numerical	Convection relies on vibration and centrifugation
Al-Rashed et al. [60]	A cover enclosure and center elliptical cylinder	Cavity angle, and nanoparticle solid volume	Numerical	The Nu rose to 45 at ϕ equal 0.2%
Daabo et al. [61]	Cylindrical cavity	Cylindrical cavity shape	Numerical	The internal height and two edges greatly impacted the heat transfer coefficient.
Hexagonal Enclosure				
Ali et al. [62]	Hexagonal cavity	Richardson number and Hartmann number	Numerical	The Hartmann and Richardson numbers affect flow structure and temperature field
Rehman et al. [63]	Hexagonal cavity	Analyse non-Newtonian fluid	Numerical	Increased Rayleigh number improves heat transport along the T-shaped fin surface
Haq et al. [64]	Hexagonal chamber	Reynolds number, Richards number, and Hartmann number	Numerical	Heat transfer significantly correlates with heat duration, Richardson number, and Reynolds number
Ghalambaz et al. [65]	Hexagonal container	Nanoparticle concentration gradient	Numerical	Increasing the magnetic number rises temperature and mass transmission.
Aly et al. [66]	Porous ring	internal double curve lengths, fusion temperature, and time parameter	Numerical	The annulus' temperature, concentration, and heat capacity circumference Cr increases with Ra
Aly et al. [67]	Wavy inner shape and hexagonal outside cavity	Partial time derivative, Darcy, Hartmann, melting temperature, Rayleigh number	Numerical	Increased Ha and decreased Da minimize nanofluid movements within the ring
Ikram et al. [68]	Hexagonal cavity	Rotor blade shape while altering Rayleigh, Reynolds, and Biot number	Numerical	Heat transfer effectiveness is conversely related to Bi and Ra and improves considerably with Reynolds numbers
Ahmed and Raizah [69]	Polygonal/polygonal or polygonal/cylinder	Thermal radiation and electromagnetic forces	Numerical	Flow area and power law control heat transfer
Rectangular Enclosure				
Elsherbiny and Ismail [70]	Rectangular enclosures	Heater position ratios and Rayleigh numbers	Numerical	Increasing Φ beyond 60° reduces Nu until it reaches its minimal value at 180°
Li and Tong [71]	Inclined rectangular chambers	Cavity's aspect ratio and inclination	Experimental & Numerical	Increasing the cavity's aspect ratio and inclination accelerates natural convection flow and convective heat transfer
Qi et al. [72]	A tiny rectangular cavity	Reynolds and Stefan's numbers	Numerical	Increasing Reynolds and Stefan numbers improve dissolution
Li et al. [73]	Rectangular chambers	Cavity height-to-width ratios	Numerical	Narrower cavities can fully use enhanced heat conductivity
Thiers et al. [74]	Rectangular cavity (modest heat engines)	Amplitude, frequency, phase shift, location	Numerical	Wave properties and vertical position of the turbulence area
Li et al. [75]	Narrow rectangular cavity	Rayleigh number, Reynolds number, and aspect ratio	Numerical	The heat transfer is affected by the change in the position of the vertical wall
Qin et al. [76]	Rectangular cavity	Reynolds number and Rayleigh number	Numerical	Different deflection profiles in the PCM melting process due to asymmetric flow barriers effect heat transport and thermal energy storage

3.2 Enclosures variable inner structures

This phase of the study includes investigations of the impact of interior bodies inside the cavity.

3.2.1 Varied inner structures in natural convection enclosures

Using numerical methods, Yoon et al. [77] calculated natural convection at Rayleigh number 107 using the temperature differential between a cold outer square cylinder and a hot inner circular cylinder. Naturally, convection in unstable zones exhibits alternating single-frequency and multi-frequency patterns. With the inner cylinder at the top, the distance between its upper surface and the container's upper surface forms a shallow layer where pure Rayleigh–Benard convection forms alternating upward and downward plumes. Hussain and Hussein [78] calculated the fixed-state heat convection of heat useful to the internal cylinder in an air-filled container with isothermal borders at a fixed temperature. It has a considerable effect on the flow pattern at high Ra but not at modest Ra. Also, the mathematical answers establish a dual cellular movement of flow amid the internal cylinder and the container. Hussein [79] simulated natural convection in a parallelogram air-filled chamber with a heated concentric circular cylinder using finite volume. The average Nusselt numbers on the inner surface of the cylinder and both sides of the bore drop as the cylinder rises and increase as it falls. Ravnik and Skerget [80] found nanofluid boosts heat transfer efficiency less when convection dominates. Tilting the casing against gravity reduces flow uniformity across the elliptical cylinder and increases heat transfer. Hatami and Safari [81] researched the convective heat transmission of nanofluids in a container with a wavy wall while inserting a heated cylinder into the hollow. The findings suggest that the cylinder's center position enhances heat transmission in both wavy side walls.

3.2.2 Varied inner structures in mixed convection enclosures

A square container with a numerically focused spinning cylinder was used by Costa and Raimundo [82] to study mixed convection. Conduction and convection heat transfer occur in the revolving drum. The findings demonstrate how the revolving cylinder impacts the case's thermal performance and how its thermophysical qualities influence heat transport. Hussain and Hussein [83] showed that increasing Richardson and Reynolds numbers affects flow and temperature fields and that rotating cylinder positions improve convective heat transfer in the square container. Roslan et al. [84] demonstrated how these factors affect heat transfer and fluid movement. Maximum heat transfer is achieved with a high nanoparticle concentration, excellent conductivity, sluggish positive circulation, and a modest cylinder size at the enclosing center. Matin and Pop [85], Selimefendigil and Öztop [86], Liao and Lin [87], and Shih and Cheng [88] studied mixed convection in the presence of different fluids and used different parameters to improve heat transfer. Selimefendigil et al. [89] numerically simulated mixed convection in a split square cavity with a copper oxide nanofluid, water, and a porous media topped with an adiabatic rotating cylinder. The forms used in the research papers are shown in Figure 6, which provides a more detailed illustration of the approach taken to investigate the interior cylinder of square cavities. Selimefendigil and Öztop [90] used finite elements to analyse nanofluid temperature transmission convection in a 3D enclosure with 2 adiabatic internal circular rolls. In average heat transfer, the copper water nanofluid with

the greatest volumetric ratio improved by 38.10% above the base fluid. Hussein et al. [91] computed two-dimensional laminar mixed convection in a trapezoidal container with a revolving inner circular cylinder and sinusoidal bottom wall. A review that focuses on enclosures that include a variety of inner structures is summarized in Table 3.
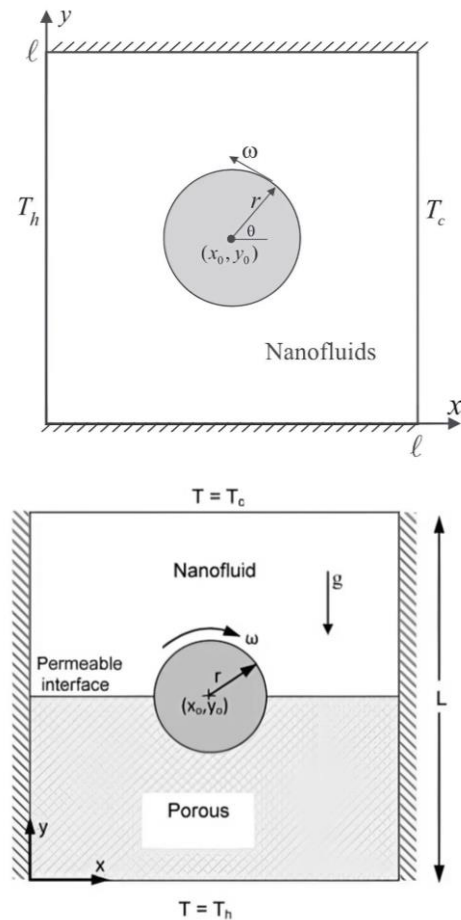
Figure 6. The physical model, including boundary conditions [84, 89]

3.3 Enclosures with fin configurations

Shi and Khodadadi [92] provided a computer analysis of the limited volume of continuous laminar natural convection within a differentially heated square cavity with a thin fin. Highly conductive thin fin connections with lengths of 20, 35, and 50% of the side were tested at seven sites on the hot left wall for $Ra=10^4$ to 10^7 and $Pr=0.707$. The flow field is amplified independent of fin length and position for large Rayleigh numbers. It also reveals that fin position and average length, Nu, Ra, are related. Khanafer et al. [93] digitally examined a thin hot wall porous fin. Ra, Da, angle, distance, and location were employed. Three fin lengths and locations were measured. Fin inclination is 30°-150°. The cavity's left wall, where fins are connected, is evenly heated but the right side is cooled. The cavity's horizontal sides are insulated. A Galerkin-based finite element formulation solves the governing equations. The permeable fin increased the Nu compared to the differentially heated enclosure for varied fin distances, locations, and inclination angles. Results show that the porous fin should be near the lowest surface or in the center of the upright warm surface at 90° for best heat transmission. Hatami's study [94] experimented to investigate heat

transmission by using heated fins inside a rectangular enclosure that was filled with nanofluids consisting of a mixture of water, titanium dioxide (TiO_2), and aluminum oxide (Al_2O_3). Furthermore, it was discovered that augmenting the heights of the fins results in a corresponding augmentation in the average Nusselt numbers. Siavashi et al. [95] digitally examined water and copper nanofluid convection in a chamber with porous fins on its heated wall. Increased fin length or number has minimal influence on Nu. Low nanoparticle

concentration improves heat transfer more than high concentrations. Entropy reduces with fin count. Saeid [96], Al-Kouz et al. [97], Al-Kouz et al. [98], and Sowmya et al. [99] studied how to optimize different fin shapes and found that the Rayleigh number enhances the velocity profile and simplifies the density function. The volume fraction of the nanoparticles affects the thermal lines. The study that focuses on enclosures that incorporate a variety of fin layouts is the subject of Table 4.

Table 3. Summary of heat transfer investigation in enclosures with different inside structures

Authors	Configuration	Main Parameters	Method	Main Results
Varied Inner Structures in Natural Convection Enclosures				
Yoon et al. [77]	Square cylinder and a hot inner circular cylinder	Internal cylinder placement	Numerical	Convection in unstable zones exhibits alternating single-frequency and multi-frequency patterns
Hussain and Hussein [78]	Inner circular cylinder in a square container	Vertical cylinder positions and Rayleigh numbers	Numerical	Establish a dual flow field between the internal cylinder and container
Hussein [79]	Chamber with a heated concentric circular cylinder	Rayleigh number, inclination angle, and vertical position	Numerical	The average Nusselt numbers on the inner surface of the cylinder and both sides of the bore drop as the cylinder rises and increase as it falls
Ravnik and Skerget [80]	Different internal bodies inside a container	Temperature differences and inclination angles	Numerical	Tilting the casing against gravity reduces flow uniformity across the elliptical cylinder and increases heat transfer.
Hatami and Safari [81]	Container with a wavy wall and a heated cylinder	Nusselt number based on the positioning of the cylinder	Numerical	The findings suggest that the cylinder's center position enhances heat transmission in both wavy side walls
Varied Inner Structures in Mixed Convection Enclosures				
Costa and Raimundo [82]	A square container with a centered cylinder	Rotation speed, thermal conductivity, and heat capacity	Numerical	The revolving cylinder impacts the case's thermal performance
Hussain and Hussein [83]	Square container with a circular cylinder	Reynolds numbers and Richardson numbers	Numerical	Increasing Richardson and Reynolds numbers affects flow and temperature fields
Roslan et al. [84]	Square container with a spinning cylinder	Cylinder radius, and angular rotation speed	Numerical	Maximum heat transfer is achieved with sluggish positive circulation and a modest cylinder size at the enclosing center
Matin and Pop [85]	A horizontal ring with inner cylinder rotation	Nanoparticle volume fraction parameter, and Rayleigh number	Numerical	In a fixed inner cylinder, the average Nusselt number grows as Ra goes from 10^3 to 10^4.
Selimefendigil and Öztop [86]	A triangular container with a spinning cylinder	Graschoff number, Hartmann number, cylinder angular rotation speed	Numerical	As cylinder angular rotation speed rises, average heat transfer and total entropy increase
Liao and Lin [87]	A square container with an active rotating cylinder	Inner cylinder-outer shell aspect ratio	Numerical	A tiny aspect ratio increases the Nusselt number ratio and heat transmission
Shih and Cheng [88]	Cavities with an internal isothermal rotating cylinder	High-viscosity fluid affects flow and temperature fields	Numerical	The triangular cavity dissipated internal heat energy best via its side walls, whereas the circular cavity performed the poorest
Selimefendigil et al. [89]	Square cavity with an adiabatic rotating cylinder	Rayleigh number, angular rotation speed	Numerical	Rayleigh number, cylinder angular rotation speed, and Darcy number increase average heat transfer
Selimefendigil and Öztop [90]	Enclosure with two internal circular rolls	Different nanoparticles	Numerical	Excellent Cu-water. Rotation direction matters. 38.10% Cu-water increase.
Hussein et al. [91]	Trapezoidal enclosure, rotating cylinder	Rayleigh, Darcy, cylinder, rotation, porous, undulation	Numerical	The copper water nanofluid with the greatest volumetric ratio improved by 38.10% above the base fluid

Table 4. Summary of the research papers of heat distribution inside enclosures with different types of fins

Authors	Configuration	Main Parameters	Method	Main Results
Shi and Khodadadi [92]	Enclosure with fins	Rayleigh number, fin length, and position	Numerical	Fin position and average length, Nu, Ra, are related
Khanafer et al. [93]	Porous fin in Square cavity	Fin inclination angle, length, and location	Numerical	The permeable fin increased Nu
Hatami's study [94]	Rectangular cavity with heated fins	Nanoparticle volume fraction and fin height	Numerical	With increasing fin heights, TiO_2 nanoparticles have high average Nusselt numbers

Siavashi et al. [95]	Cavity with an array of porous fins	Fin number and length, Rayleigh number, and Darcy number	Numerical	Porous fins with a high Darcy number promote heat transmission
Saeid [96]	Fin shapes heated a square chamber	Graschoff number and total fin area	Numerical	Heat transmission may be improved by increasing the Graschoff number or fin height
Al-Kouz et al. [97]	Chamber with solid hot wall fins	Conductivity ratio, fin porosity, and inclination angle	Numerical	Porous fins surpass solid fins in heat transmission
Al-Kouz et al. [98]	Square cavity with two solid fins	Knudson number (Kn), Rayleigh number (Ra)	Numerical	Kn directly inversely affects entropy generation
Sowmya et al. [99]	Rectangular chamber with two heated fins	Ra and Ha	Numerical	Laminar movement is observable at lesser Ra and higher Ha, whereas turbulent movement is apparent at higher Rayleigh numbers and lesser Hartmann numbers

3.4 Experimental studies on enclosures with fins

Hu et al. [100] examined the water nanofluid Al_2O_3 thermal conductivity and viscosity in a square container to study heat transmission. The driving force of temperature difference contributes most to the nanoparticle concentration. Solomon et al. [101] found the Rayleigh number strongly affects nanofluid buoyancy and Nusselt number. Chen et al. [102] examined natural convection in a heated chamber with a horizontal fin on a heated sidewall to determine how fin location and beginning temperature affected air temperature, velocity profiles, fin surface temperature, and fin heat transfer coefficient. Fin location affects the flow field. Hence, it cannot be disregarded. Joneidi et al. [103] found that additional fins give a more uniform temperature distribution, which enhances melting more than other parameters. It was also found that additional fins regulate heat sink base plate temperature better at lower critical temperatures. Abdulsahib and Al-Farhany [104] calculated mixed heat transmission in a two-layer container. Findings demonstrated uniform temperature distribution in the top half of the enclosure and concentration along the hot wall at the bottom. Anticlockwise spin reduced the circular cylinder's bottom and left top temperature. Abdi and Rastan [105] examined three fin designs with varied lengths and numbers in horizontal, inclined, and vertical orientations in a rectangular hollow. The limited mode fins do not impede buoyancy-dependent structures in these orientations. Close contact melting is only slightly affected by fin count. However, lengthening the fins is more promising for a solid, long-lasting connection. Figure 7 is an illustration of the scientific devices that were used in the research papers that are included in this part. The purpose of this illustration is to make the study concept more understandable in terms of the variety of devices utilized in scientific investigations.
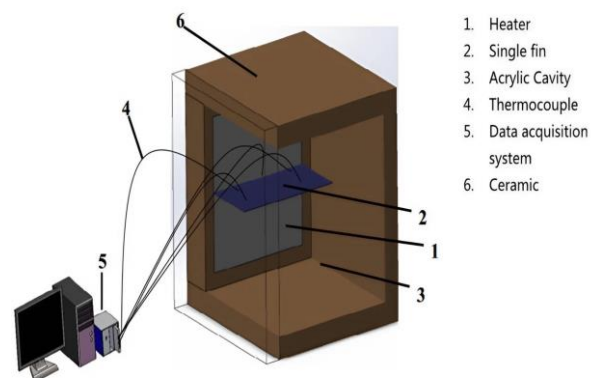
Figure 7. Experimental designs of enclosures [100, 102]

4. CONCLUSIONS

The present provided a comprehensive review of previous investigations that examined the thermal design of heat sinks and studies of heat transport inside various cavities. Research studies conducted on the thermal design of heat sinks provide a summary of the use of natural convection as a means of heat dissipation and explain the impact of various fin shapes and orientations on the efficiency and performance of heat sinks. How multiple mechanisms for input and output influence the efficiency of the heat sinks and their performance. Additionally, the utilization of materials such as nanofluid, copper metal foam, and graphene to enhance heat transfer, the utilization of FPFHS and PFHS fins within the heat sink, the utilization of porous microchannel flow to improve the efficiency of the system, and the investigation of various working fluids to enhance the heat sink are all explored as examples of strategies that have been implemented. It is also concluded that heat sinks with double-layered microchannels are superior in engineering applications compared to a single layer.

In addition, a summary of the research articles that investigated heat transfer within cavities is provided. These studies include cavities with various geometric forms, such as circular, cylindrical, hexagonal, and rectangular, and containers with different interior designs that use natural and mixed convection. In addition to enclosures with various fin designs, experimental investigations have also been conducted on enclosures with various fin settings. Considering everything, the findings shed light on many elements of heat transfer in multiple cavity shapes and provide us with valuable
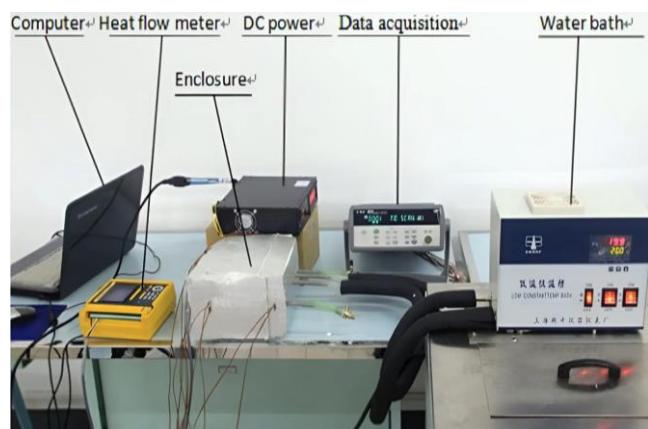
knowledge that can be used to improve the efficiency of heat transfer processes in these kinds of systems.

Prior research has mainly concentrated on examining the thermodynamics of the heat sink and the cavities as independent entities, disregarding the possible benefits of incorporating heat sinks inside the cavities. Hence, this pioneering research project suggests that future investigations might focus on a more detailed analysis of heat flow inside the packages when the heat sink is present, enabling possible enhancements regarding heat transport efficiency.

Concluded that heat transfer improvements in heat sinks, such as the use of fin shapes and directions, the use of a fluid such as nanofluid, as well as the use of porous materials, can be applied in the existence of cavities of varying geometric forms and the use of natural and mixed convection to rise the efficiency the transfer of heat.

REFERENCES

[1] Lee, H. (2022). Thermal Design: Heat Sinks, Thermoelectrics, Heat Pipes, Compact Heat Exchangers, and Solar Cells. John Wiley & Sons. http://doi.org/10.1002/9781119686040

[2] Ahmed, H.E., Salman, B., Kherbeet, A.S., Ahmed, M. (2018). Optimization of thermal design of heat sinks: A review. International Journal of Heat and Mass Transfer, 118: 129-153. http://doi.org/10.1016/j.ijheatmasstransfer.2017.10.099

[3] Safari, V., Kamkari, B., Zandimagham, M., Hewitt, N. (2023). Transient thermal behavior of a passive heat sink integrated with phase change material: A numerical simulation. International Journal of Thermofluids, 20: 100454. http://doi.org/10.1016/j.ijft.2023.100454

[4] Narendran, G., Gnanasekaran, N., Perumal, D.A. (2018). A review on recent advances in microchannel heat sink configurations. Recent Patents on Mechanical Engineering, 11(3): 190-215. http://doi.org/10.2174/2212797611666180726124047

[5] Al-Omari, S.A.B., Mahmoud, F., Qureshi, Z.A., Elnajjar, E. (2023). The impact of different fin configurations and design parameters on the performance of a finned PCM heat sink. International Journal of Thermofluids, 20: 100476. http://doi.org/10.1016/j.ijft.2023.100476

[6] Alihosseini, Y., Targhi, M.Z., Heyhat, M.M., Ghorbani, N. (2020). Effect of a micro heat sink geometric design on thermo-hydraulic performance: A review. Applied Thermal Engineering, 170: 114974. http://doi.org/10.1016/j.applthermaleng.2020.114974

[7] Mostafa, Y.T., El-Dosoky, M.F., Abdelgawad, M., Hassan, O. (2023). Numerical investigation of a hybrid double layer microchannel heat sink with jet impingement. International Journal of Thermofluids, 20: 100465. http://doi.org/10.1016/j.ijft.2023.100465

[8] Dhaiban, H.T., Hussein, M.A. (2020). The optimal design of heat sinks: A review. Journal of Applied and Computational Mechanics, 6(4): 1030-1043. http://doi.org/10.22055/jacm.2019.14852

[9] Chingulpitak, S., Wongwises, S. (2015). A review of the effect of flow directions and behaviors on the thermal performance of conventional heat sinks. International Journal of Heat and Mass Transfer, 81: 10-18. http://doi.org/10.1016/j.ijheatmasstransfer.2014.09.081

[10] Jeng, T.M., Tzeng, S.C. (2014). Heat transfer measurement of the cylindrical heat sink with sintered-metal-bead-layers fins and a built-in motor fan. International Communications in Heat and Mass Transfer, 59: 136-142. http://doi.org/10.1016/j.icheatmasstransfer.2014.10.006

[11] Liu, Y., Chen, H., Zhang, H., Li, Y. (2015). Heat transfer performance of lotus-type porous copper heat sink with liquid GaInSn coolant. International Journal of Heat and Mass Transfer, 80: 605-613. http://doi.org/10.1016/j.ijheatmasstransfer.2014.09.058

[12] Abdulkadhim, A., Abed, I.M., Mahjoub Said, N. (2021). Review of natural convection within various shapes of enclosures. Arabian Journal for Science and Engineering, 46: 11543-11586. http://doi.org/10.1007/s13369-021-05952-6

[13] Rashid, F.L., Hussein, A.K., Malekshah, E.H., Abderrahmane, A., Guedri, K., Younis, O. (2022). Review of heat transfer analysis in different cavity geometries with and without nanofluids. Nanomaterials, 12(14): 2481. http://doi.org/10.3390/nano12142481

[14] Abdulkadhim, A., Mejbel Abed, I., Mahjoub Said, N. (2021). An exhaustive review on natural convection within complex enclosures: Influence of various parameters. Chinese Journal of Physics, 74: 365-388. http://doi.org/10.1016/j.cjph.2021.10.012

[15] Saha, G., Al-Waaly, A.A., Ikram, M.M., Bihani, R., Saha, S.C. (2024). Unveiling the dynamics of entropy generation in enclosures: A systematic review. International Journal of Thermofluids, 21: 100568. http://doi.org/10.1016/j.ijft.2024.100568

[16] Alomari, M.A., Al-Farhany, K., Al-Salami, Q.H., Ali, I., Biswas, N., Mohamed, M.H., Alqurashi, F. (2024). Numerical analysis to investigate the effect of a porous block on MHD mixed convection in a split lid-driven cavity with nanofluid. International Journal of Thermofluids, 22: 100621. http://doi.org/10.1016/j.ijft.2024.100621

[17] Abood, F.A., Yaseen, S.J., Mohammed, I.G., Homod, R.Z., Mohammed, H.I. (2024). Enhancing thermal performance in a magnetized square cavity: Novel insights from mixed convection of Ag-MgO nanofluid around a rotating cylinder. International Journal of Thermofluids, 22: 100630. http://doi.org/10.1016/j.ijft.2024.100630

[18] Abdulsahib, A.D., Al-Farhany, K. (2021). Review of the effects of stationary/rotating cylinder in a cavity on the convection heat transfer in porous media with/without nanofluid. Mathematical Modelling of Engineering Problems, 8(3): 356-364. https://doi.org/10.18280/mmep.080304

[19] Abdulsahib, A.D., Hashim, A.S., Al-Farhany, K., Abdulkadhim, A., Mebarek-Oudina, F. (2022). Natural convection investigation under influence of internal bodies within a nanofluid-filled square cavity. The European Physical Journal Special Topics, 231(13-14): 2605-2621. http://doi.org/10.1140/epjs/s11734-022-00584-9

[20] Alshare, A., Abderrahmane, A., Guedri, K., Younis, O., Fayz-Al-Asad, M., Ali, H.M., Al-Kouz, W. (2022). Hydrothermal and entropy investigation of nanofluid natural convection in a lid-driven Cavity concentric with an elliptical cavity with a wavy boundary heated from below. Nanomaterials, 12(9): 1392. http://doi.org/10.3390/nano12091392

[21] Tari, I., Mehrtash, M. (2013). Natural convection heat transfer from horizontal and slightly inclined plate-fin heat sinks. Applied Thermal Engineering, 61(2): 728-736. http://doi.org/10.1016/j.applthermaleng.2013.09.003

[22] Tari, I., Mehrtash, M. (2013). Natural convection heat transfer from inclined plate-fin heat sinks. International Journal of Heat and Mass Transfer, 56(1-2): 574-593. https://doi.org/10.1016/j.ijheatmasstransfer.2012.08.050

[23] Jang, D., Park, S.J., Yook, S.J., Lee, K.S. (2014). The orientation effect for cylindrical heat sinks with application to LED light bulbs. International Journal of Heat and Mass Transfer, 71: 496-502. http://doi.org/10.1016/j.ijheatmasstransfer.2013.12.037

[24] Muneeshwaran, M., Tsai, M.K., Wang, C.C. (2023). Heat transfer augmentation of natural convection heat sink through notched fin design. International Communications in Heat and Mass Transfer, 142: 106676. http://doi.org/10.1016/j.icheatmasstransfer.2023.106676

[25] Hung, T.C., Yan, W.M. (2012). Effects of tapered-channel design on thermal performance of microchannel heat sink. International Communications in Heat and Mass Transfer, 39(9): 1342-1347. http://doi.org/10.1016/j.icheatmasstransfer.2012.08.008

[26] Costa, V.A., Lopes, A.M. (2014). Improved radial heat sink for led lamp cooling. Applied Thermal Engineering, 70(1): 131-138. http://doi.org/10.1016/j.applthermaleng.2014.04.068

[27] Kim, D.K. (2014). Thermal optimization of branched-fin heat sinks subject to a parallel flow. International Journal of Heat and Mass Transfer, 77: 278-287. http://doi.org/10.1016/j.ijheatmasstransfer.2014.05.010

[28] Türkakar, G., Okutucu-Özyurt, T. (2012). Dimensional optimization of microchannel heat sinks with multiple heat sources. International Journal of Thermal Sciences, 62: 85-92. http://doi.org/10.1016/j.ijthermalsci.2011.12.015

[29] Shahsavar, A., Farhadi, P., Yıldız, Ç., Moradi, M., Arıcı, M. (2022). Evaluation of entropy generation characteristics of boehmite-alumina nanofluid with different shapes of nanoparticles in a helical heat sink. International Journal of Mechanical Sciences, 225: 107338. http://doi.org/10.1016/j.ijmecsci.2022.107338

[30] Vinodhan, V.L., Rajan, K. (2014). Computational analysis of new microchannel heat sink configurations. Energy Conversion and Management, 86: 595-604. http://doi.org/10.1016/j.enconman.2014.06.038

[31] Xia, G., Jiang, J., Wang, J., Zhai, Y., Ma, D. (2015). Effects of different geometric structures on fluid flow and heat transfer performance in microchannel heat sinks. International Journal of Heat and Mass Transfer, 80: 439-447. http://doi.org/10.1016/j.ijheatmasstransfer.2014.08.095

[32] Al-Hasani, H.M., Freegah, B. (2022). Influence of fluid inlet–outlet on hydrothermal evaluation for different serpentine mini-channel heat sink configurations. Heat Transfer, 51(8): 7635-7654,2022. http://doi.org/10.1002/htj.22659

[33] Mohammed, H., Gunnasegaran, P., Shuaib, N. (2011). Influence of various base nanofluids and substrate materials on heat transfer in trapezoidal microchannel heat sinks. International Communications in Heat and Mass Transfer, 38(2): 194-201. http://doi.org/10.1016/j.icheatmasstransfer.2010.12.010

[34] Qu, Z., Li, W., Wang, J., Tao, W. (2012). Passive thermal management using metal foam saturated with phase change material in a heat sink. International Communications in Heat and Mass Transfer, 39(10): 1546-1549. http://doi.org/10.1016/j.icheatmasstransfer.2012.09.001

[35] Shkarah, A.J., Sulaiman, M.Y.B., Ayob, M.R.B.H., Togun, H. (2013). A 3D numerical study of heat transfer in a single-phase micro-channel heat sink using graphene, aluminum and silicon as substrates. International Communications in Heat and Mass Transfer, 48: 108-115. http://doi.org/10.1016/j.icheatmasstransfer.2013.08.006

[36] Lin, S.C., Chuang, F.S., Chou, C.A. (2005). Experimental study of the heat sink assembly with oblique straight fins. Experimental Thermal and Fluid Science, 29(5): 591-600. http://doi.org/10.1016/j.expthermflusci.2004.08.003

[37] Zhao, J., Huang, S., Gong, L., Huang, Z. (2016). Numerical study and optimizing on micro square pin-fin heat sink for electronic cooling. Applied Thermal Engineering, 93: 1347-1359. http://doi.org/10.1016/j.applthermaleng.2015.08.105

[38] Al-Sallami, W., Al-Damook, A., Thompson, H. (2016). A numerical investigation of thermal airflows over strip fin heat sinks. International Communications in Heat and Mass Transfer, 75: 183-191. http://doi.org/10.1016/j.icheatmasstransfer.2016.03.014

[39] Hung, T.C., Huang, Y.X., Yan, W.M. (2013). Thermal performance of porous microchannel heat sink: Effects of enlarging channel outlet. International Communications in Heat and Mass Transfer, 48: 86-92. http://doi.org/10.1016/j.icheatmasstransfer.2013.08.001

[40] Zhang, H., Chen, L., Liu, Y., Li, Y. (2013). Experimental study on heat transfer performance of lotus-type porous copper heat sink. International Journal of Heat and Mass Transfer, 56(1-2): 172-180. http://doi.org/10.1016/j.ijheatmasstransfer.2012.08.047

[41] Deng, D., Tang, Y., Liang, D., He, H., Yang, S. (2014). Flow boiling characteristics in porous heat sink with reentrant microchannels. International Journal of Heat and Mass Transfer, 70: 463-477. http://doi.org/10.1016/j.ijheatmasstransfer.2013.10.057

[42] Abdollahi, S., Jalili, P., Jalili, B., Nourozpour, H., Safari, Y., Pasha, P., Ganji, D. (2023). Computer simulation of Cu: AlOOH/water in a microchannel heat sink using a porous media technique and solved by numerical analysis AGM and FEM. Theoretical and Applied Mechanics Letters, 13(3): 100432. http://doi.org/10.1016/j.taml.2023.100432

[43] Ho, C.J., Chen, W. (2013). An experimental study on thermal performance of Al_2O_3/water nanofluid in a minichannel heat sink. Applied Thermal Engineering, 50(1): 516-522. http://doi.org/10.1016/j.applthermaleng.2012.07.037

[44] Moraveji, M.K., Ardehali, R.M., Ijam, A. (2013). CFD investigation of nanofluid effects (cooling performance and pressure drop) in mini-channel heat sink. International Communications in Heat and Mass Transfer, 40: 58-66. https://doi.org/10.1016/j.icheatmasstransfer.2012.10.021

[45] Moraveji, M.K., Ardehali, R.M. (2013). CFD modeling (comparing single and two-phase approaches) on thermal performance of Al_2O_3/water nanofluid in mini-channel

heat sink. International Communications in Heat and Mass Transfer, 44: 157-164. http://doi.org/10.1016/j.icheatmasstransfer.2013.02.012

[46] Ho, C.J., Chen, W.C., Yan, W.M. (2014). Correlations of heat transfer effectiveness in a minichannel heat sink with water-based suspensions of Al_2O_3 nanoparticles and/or MEPCM particles. International Journal of Heat and Mass Transfer, 69: 293-299. http://doi.org/10.1016/j.ijheatmasstransfer.2013.10.030

[47] Naphon, P., Nakharintr, L. (2015). Turbulent two phase approach model for the nanofluids heat transfer analysis flowing through the minichannel heat sinks. International Journal of Heat and Mass Transfer, 82: 388-395. http://doi.org/10.1016/j.ijheatmasstransfer.2014.11.024

[48] Shao, B., Wang, L., Cheng, H., Li, J. (2012). Optimization and numerical simulation of multi-layer microchannel heat sink. Procedia Engineering, 31: 928-933. http://doi.org/10.1016/j.proeng.2012.01.1123

[49] Wong, K.C., Muezzin, F.N.A. (2013). Heat transfer of a parallel flow two-layered microchannel heat sink. International Communications in Heat and Mass Transfer, 49: 136-140. http://doi.org/10.1016/j.icheatmasstransfer.2013.09.004

[50] Ahmed, H.E., Ahmed, M., Seder, I.M., Salman, B. (2016). Experimental investigation for sequential triangular double-layered microchannel heat sink with nanofluids. International Communications in Heat and Mass Transfer, 77: 104-115. http://doi.org/10.1016/j.icheatmasstransfer.2016.06.010

[51] Ho, C., Peng, J.K., Yang, T.F., Rashidi, S., Yan, W.M. (2023). Comparison of cooling performance of nanofluid flows in mini/micro-channel stacked double-layer heat sink and single-layer micro-channel heat sink. International Journal of Thermal Sciences, 191: 108375. http://doi.org/10.1016/j.ijthermalsci.2023.108375

[52] Hatami, M., Song, D., Jing, D. (2016). Optimization of a circular-wavy cavity filled by nanofluid under the natural convection heat transfer condition. International Journal of Heat and Mass Transfer, 98: 758-767. http://doi.org/10.1016/j.ijheatmasstransfer.2016.03.063

[53] Hadavand, M., Yousefzadeh, S., Akbari, O.A., Pourfattah, F., Nguyen, H.M., Asadi, A. (2019). A numerical investigation on the effects of mixed convection of Ag-water nanofluid inside a sim-circular lid-driven cavity on the temperature of an electronic silicon chip. Applied Thermal Engineering, 162: 114298. http://doi.org/10.1016/j.applthermaleng.2019.114298

[54] Sheikholeslami, M., Mehryan, S., Shafee, A., Sheremet, M.A. (2019). Variable magnetic forces impact on magnetizable hybrid nanofluid heat transfer through a circular cavity. Journal of Molecular Liquids, 277: 388-396. http://doi.org/10.1016/j.molliq.2018.12.104

[55] Gangawane, K.M., Oztop, H.F. (2020). Mixed convection in the heated semi-circular lid-driven cavity for non-Newtonian power-law fluids: Effect of presence and shape of the block. Chinese Journal of Chemical Engineering, 28(5): 1225-1240. http://doi.org/10.1016/j.cjche.2020.03.005

[56] Shahrestani, A.B., Alshuraiaan, B., Izadi, M. (2021). Combined natural convection-FSI inside a circular enclosure divided by a movable barrier. International Communications in Heat and Mass Transfer, 126: 105426.

http://doi.org/10.1016/j.icheatmasstransfer.2021.105426

[57] Shen, Z.G., Wu, S.Y., Xiao, L. (2016). Numerical study of wind effects on combined convective heat loss from an upward-facing cylindrical cavity. Solar Energy, 132: 294-309. http://doi.org/10.1016/j.solener.2016.03.021

[58] Bouhal, T., Kousksou, T., Jamil, A. (2018). CFD thermal energy storage enhancement of PCM filling a cylindrical cavity equipped with submerged heating sources. Journal of Energy Storage, 18: 360-370. http://doi.org/10.1016/j.est.2018.05.015

[59] Vjatkin, A., Kozlov, V., Sabirov, R. (2019). Convection of a heat-generating fluid in a rotating cylindrical cavity subject to transverse vibrations. International Journal of Thermal Sciences, 137: 560-570. http://doi.org/10.1016/j.ijthermalsci.2018.12.008

[60] Al-Rashed, A.A., Shahsavar, A., Akbari, M., Toghraie, D., Akbari, M., Afrand, M. (2019). Finite volume simulation of mixed convection in an inclined lid-driven cavity filled with nanofluids: effects of a hot elliptical centric cylinder, cavity angle and volume fraction of nanoparticles. Physica A: Statistical Mechanics and its Applications, 527: 121122. http://doi.org/10.1016/j.physa.2019.121122

[61] Daabo, A.M., Al-Mola, Y.S., Al-Rawy, A.Y., Lattimore, T. (2019). State of the art single-objective optimization of small scale cylindrical cavity receiver. Sustainable Energy Technologies and Assessments, 35: 278-290. http://doi.org/10.1016/j.seta.2019.07.009

[62] Ali, M.M., Alim, M., Ahmed, S.S. (2017). Magnetohydrodynamic mixed convection flow in a hexagonal enclosure. Procedia Engineering, 194: 479-486. http://doi.org/10.1016/j.proeng.2017.08.174

[63] Rehman, K.U., Malik, M., Al-Mdallal, Q.M., Al-Kouz, W. (2020). Heat transfer analysis on buoyantly convective non-Newtonian stream in a hexagonal enclosure rooted with T-Shaped flipper: hybrid meshed analysis. Case Studies in Thermal Engineering, 21: 100725. http://doi.org/10.1016/j.csite.2020.100725

[64] Haq, R.U., Soomro, F.A., Wang, X., Tlili, I. (2020). Partially heated lid-driven flow in a hexagonal cavity with inner circular obstacle via FEM. International Communications in Heat and Mass Transfer, 117: 104732.
http://doi.org/10.1016/j.icheatmasstransfer.2020.104732

[65] Ghalambaz, M., Sabour, M., Sazgara, S., Pop, I., Trâmbiţaş, R. (2020). Insight into the dynamics of ferrohydrodynamic (FHD) and magnetohydrodynamic (MHD) nanofluids inside a hexagonal cavity in the presence of a non-uniform magnetic field. Journal of Magnetism and Magnetic Materials, 497: 166024. http://doi.org/10.1016/j.jmmm.2019.166024

[66] Aly, A.M., Al-Hanaya, A., Raizah, Z. (2021). The magnetic power on natural convection of NEPCM suspended in a porous annulus between a hexagonal-shaped cavity and dual curves. Case Studies in Thermal Engineering, 28: 101354,2021. http://doi.org/10.1016/j.csite.2021.101354

[67] Aly, A.M., Raizah, Z., Al-Hanaya, A. (2021). Double rotations between an inner wavy shape and a hexagonal-shaped cavity suspended by NEPCM using a time-fractional derivative of the ISPH method. International Communications in Heat and Mass Transfer, 127: 105533.
http://doi.org/10.1016/j.icheatmasstransfer.2021.105533

[68] Ikram, M.M., Saha, G., Saha, S.C. (2021). Conjugate forced convection transient flow and heat transfer analysis in a hexagonal, partitioned, air filled cavity with dynamic modulator. International Journal of Heat and Mass Transfer, 167: 120786,2021. http://doi.org/10.1016/j.ijheatmasstransfer.2020.120786

[69] Ahmed, S.E., Raizah, Z.A. (2022). FEM treatments for MHD radiative convective flow of MWCNTs $C_2H_6O_2$ nanofluids between inclined hexagonal/hexagonal or hexagonal/cylinder. Ain Shams Engineering Journal, 13(2): 101549. http://doi.org/10.1016/j.asej.2021.07.003

[70] Elsherbiny, S.M., Ismail, O.I. (2015). Heat transfer in inclined air rectangular cavities with two localized heat sources. Alexandria Engineering Journal, 54(4): 917-927. http://doi.org/10.1016/j.aej.2015.07.013

[71] Li, H., Tong, S. (2016). Natural convective heat transfer in the inclined rectangular cavities with low width-to-height ratios. International Journal of Heat and Mass Transfer, 93: 398-407. http://doi.org/10.1016/j.ijheatmasstransfer.2015.10.027

[72] Qi, R., Wang, Z., Ren, J., Wu, Y. (2020). Numerical investigation on heat transfer characteristics during melting of lauric acid in a slender rectangular cavity with flow boundary condition. International Journal of Heat and Mass Transfer, 157: 119927. http://doi.org/10.1016/j.ijheatmasstransfer.2020.119927

[73] Li, Z.R., Hu, N., Liu, J., Zhang, R.H., Fan, L.W. (2020). Revisiting melting heat transfer of nano-enhanced phase change materials (NePCM) in differentially-heated rectangular cavities using thermochromic liquid crystal (TLC) thermography. International Journal of Heat and Mass Transfer, 159: 120119. http://doi.org/10.1016/j.ijheatmasstransfer.2020.120119

[74] Thiers, N., Gers, R., Skurtys, O. (2020). Heat transfer enhancement by localised time varying thermal perturbations at hot and cold walls in a rectangular differentially heated cavity. International Journal of Thermal Sciences, 151: 106245. http://doi.org/10.1016/j.ijthermalsci.2019.106245

[75] Li, P., Wang, Z., Liu, Z., Heng, W., Qin, H. (2021). Convective heat transfer mechanisms of molten phase change material in a vertical slender rectangular cavity: A numerical case study. Case Studies in Thermal Engineering, 26: 101139. http://doi.org/10.1016/j.csite.2021.101139

[76] Qin, H., Wang, Z., Heng, W., Liu, Z., Li, P. (2021). Numerical study of melting and heat transfer of PCM in a rectangular cavity with bilateral flow boundary conditions. Case Studies in Thermal Engineering, 27: 101183. http://doi.org/10.1016/j.csite.2021.101183

[77] Yoon, H.S., Ha, M.Y., Kim, B.S., Yu, D.H. (2009). Effect of the position of a circular cylinder in a square enclosure on natural convection at Rayleigh number of 107. Physics of Fluids, 21(4): 047101. http://doi.org/10.1063/1.3112735

[78] Hussain, S.H., Hussein, A.K. (2010). Numerical investigation of natural convection phenomena in a uniformly heated circular cylinder immersed in square enclosure filled with air at different vertical locations. International Communications in Heat and Mass Transfer, 37(8): 1115-1126. http://doi.org/10.1016/j.icheatmasstransfer.2010.05.016

[79] Hussein, A.K. (2013). Computational analysis of natural convection in a parallelogrammic cavity with a hot concentric circular cylinder moving at different vertical locations. International Communications in Heat and Mass Transfer, 46: 126-133. http://doi.org/10.1016/j.icheatmasstransfer.2013.05.008

[80] Ravnik, J., Škerget, L. (2015). A numerical study of nanofluid natural convection in a cubic enclosure with a circular and an ellipsoidal cylinder. International Journal of Heat and Mass Transfer, 89: 596-605. http://doi.org/10.1016/j.ijheatmasstransfer.2015.05.089

[81] Hatami, M., Safari, H. (2016). Effect of inside heated cylinder on the natural convection heat transfer of nanofluids in a wavy-wall enclosure. International Journal of Heat and Mass Transfer, 103: 1053-1057. http://doi.org/10.1016/j.ijheatmasstransfer.2016.08.029

[82] Costa, V., Raimundo, A. (2010). Steady mixed convection in a differentially heated square enclosure with an active rotating circular cylinder. International Journal of Heat and Mass Transfer, 53(5-6): 1208-1219. http://doi.org/10.1016/j.ijheatmasstransfer.2009.10.007

[83] Hussain, S.H., Hussein, A.K. (2011). Mixed convection heat transfer in a differentially heated square enclosure with a conductive rotating circular cylinder at different vertical locations. International Communications in Heat and Mass Transfer, 38(2): 263-274. http://doi.org/10.1016/j.icheatmasstransfer.2010.12.006

[84] Roslan, R., Saleh, H., Hashim, I. (2012). Effect of rotating cylinder on heat transfer in a square enclosure filled with nanofluids. International Journal of Heat and Mass Transfer, 55(23-24): 7247-7256. http://doi.org/10.1016/j.ijheatmasstransfer.2012.07.051

[85] Matin, M.H., Pop, I. (2014). Numerical study of mixed convection heat transfer of a nanofluid in an eccentric annulus. Numerical Heat Transfer, Part A: Applications, 65(1): 84-105. http://doi.org/10.1080/10407782.2013.812000

[86] Selimefendigil, F., Öztop, H.F. (2014). MHD mixed convection of nanofluid filled partially heated triangular enclosure with a rotating adiabatic cylinder. Journal of the Taiwan Institute of Chemical Engineers, 45(5): 2150-2162. http://doi.org/10.1016/j.jtice.2014.06.018

[87] Liao, C.C., Lin, C.A. (2014). Mixed convection of a heated rotating cylinder in a square enclosure. International Journal of Heat and Mass Transfer, 72: 9-22. http://doi.org/10.1016/j.ijheatmasstransfer.2013.12.081

[88] Shih, Y.C., Cheng, Y.J. (2015). The effect of viscous dissipation on heat transfer in cavities of varying shape due to an inner rotating circular cylinder. Numerical Heat Transfer, Part A: Applications, 68(2): 150-173. http://doi.org/10.1080/10407782.2014.977134

[89] Selimefendigil, F., Ismael, M.A., Chamkha, A.J. (2017). Mixed convection in superposed nanofluid and porous layers in square enclosure with inner rotating cylinder. International Journal of Mechanical Sciences, 124: 95-108. http://doi.org/10.1016/j.ijmecsci.2017.03.007

[90] Selimefendigil, F., Öztop, H.F. (2018). Mixed convection of nanofluids in a three dimensional cavity with two adiabatic inner rotating cylinders. International Journal of Heat and Mass Transfer, 117: 331-343. https://doi.org/10.1016/j.ijmecsci.2017.03.007

[91] Hussein, A.K., Hamzah, H.K., Ali, F.H., Kolsi, L. (2019). Mixed convection in a trapezoidal enclosure filled with two layers of nanofluid and porous media with a rotating circular cylinder and a sinusoidal bottom wall. Journal of

Thermal Analysis and Calorimetry, 141: 2061-2079. http://doi.org/10.1007/s10973-019-08963-6

[92] Shi, X., Khodadadi, J. (2003). Laminar natural convection heat transfer in a differentially heated square cavity due to a thin fin on the hot wall. Journal of Heat and Mass Transfer, 125(4): 624-634. http://doi.org/10.1115/1.1571847

[93] Khanafer, K., AlAmiri, A., Bull, J. (2015). Laminar natural convection heat transfer in a differentially heated cavity with a thin porous fin attached to the hot wall. International Journal of Heat and Mass Transfer, 87: 59-70. http://doi.org/10.1016/j.ijheatmasstransfer.2015.03.077

[94] Hatami, M. (2017). Numerical study of nanofluids natural convection in a rectangular cavity including heated fins. Journal of Molecular Liquids, 233: 1-8. http://doi.org/10.1016/j.molliq.2017.02.112

[95] Siavashi, M., Yousofvand, R., Rezanejad, S. (2018). Nanofluid and porous fins effect on natural convection and entropy generation of flow inside a cavity. Advanced Powder Technology, 29(1): 142-156. http://doi.org/10.1016/j.apt.2017.10.021

[96] Saeid, N.H. (2018). Natural convection in a square cavity with discrete heating at the bottom with different fin shapes. Heat Transfer Engineering, 39(2): 154-161. http://doi.org/10.1080/01457632.2017.1288053

[97] Al-Kouz, W., Alshare, A., Kiwan, S., Al-Muhtady, A., Alkhalidi, A., Saadeh, H. (2018). Two-dimensional analysis of low-pressure flows in an inclined square cavity with two fins attached to the hot wall. International Journal of Thermal Sciences, 126: 181-193. http://doi.org/10.1016/j.ijthermalsci.2018.01.005

[98] Al-Kouz, W., Al-Muhtady, A., Owhaib, W., Al-Dahidi, S., Hader, M., Abu-Alghanam, R. (2019). Entropy generation optimization for rarified nanofluid flows in a square cavity with two fins at the hot wall. Entropy, 21(2): 103. http://doi.org/10.3390/e21020103

[99] Sowmya, G., Gireesha, B., Animasaun, I., Shah, N.A. (2021). Significance of buoyancy and Lorentz forces on water-conveying iron (III) oxide and silver nanoparticles in a rectangular cavity mounted with two heated fins: heat transfer analysis. Journal of Thermal Analysis and Calorimetry, 144(6): 2369-2384. http://doi.org/10.1007/s10973-021-10550-7

[100] Hu, Y., He, Y., Qi, C., Jiang, B., Schlaberg, H.I. (2014). Experimental and numerical study of natural convection in a square enclosure filled with nanofluid. International Journal of Heat and Mass Transfer, 78: 380-392. http://doi.org/10.1016/j.ijheatmasstransfer.2014.07.001

[101] Solomon, A.B., van Rooyen, J., Rencken, M., Sharifpur, M., Meyer, J.P. (2017). Experimental study on the influence of the aspect ratio of square cavity on natural convection heat transfer with Al₂O₃/Water nanofluids. International Communications in Heat and Mass Transfer, 88: 254-261. https://doi.org/10.1016/j.icheatmasstransfer.2017.09.007

[102] Chen, H.T., Lin, M.C., Chang, J.R. (2018). Numerical and experimental studies of natural convection in a heated cavity with a horizontal fin on a hot sidewall. International Journal of Heat and Mass Transfer, 124: 1217-1229. http://doi.org/10.1016/j.ijheatmasstransfer.2018.04.046

[103] Joneidi, M., Rahimi, M., Pakrouh, R., Bahrampoury, R. (2020). Experimental analysis of Transient melting process in a horizontal cavity with different configurations of fins. Renewable Energy, 145: 2451-2462. http://doi.org/10.1016/j.renene.2019.07.114

[104] Abdulsahib, A.D., Al-Farhany, K. (2020). Experimental investigation of mixed convection on a rotating circular cylinder in a cavity filled with nanofluid and porous media. Al-Qadisiyah Journal for Engineering Sciences, 13(2): 99-108. http://doi.org/10.30772/qjes.v13i2.653

[105] Abdi, A., Rastan, H. (2023). Experimental comparative analysis of close-contact and constrained melting of n-eicosane in a finned rectangular cavity. Applied Thermal Engineering, 219: 119677. http://doi.org/10.1016/j.applthermaleng.2022.119677

NOMENCLATURE

AR	aspect ratio
Nr	number of ratios
CFD	computational fluid dynamics
FEM	finite element method
FHD	ferro-hydrodynamic
LED	Light-emitting diode
CPU	central processing unit
DLMCHS	double-layer micro-channel heat sink
MCHS	microchannel heat sink
FPF	flat-plate fin
mPCM	molten phase change material
HS	heat sink
N_F	nanofluid
PF	pin-fin
MHD	magneto hydrodynamic
Mnf	magnetic number
MWCNT	multi-wall carbon nanotubes
ΔT	temperature difference
PCM	phase change material
Nu	Nusselt number
Bi	Biot number
Le	Lewis number
Ha	Hartmann number
Pr	Prandtl number
Ra	Rayleigh number
Ri	Richardson number
Re	Reynolds number
Da	darcy number
Kn	Knudson number
θ	cavity angle
ϕ	solid nanoparticle percentage